V European Conference on Computational Fluid Dynamics
ECCOMAS CFD 2010
W.H.Zhao and X.F.Wang
Lisbon, Portugal, 14-17 June 2010

NON-NEWTONIAN BEHAVIOR OF BLOOD AND ARTERIAL CURVATURE INFLUENCE VARIATIONS OF WALL SHEAR STRESS IN STENTED ARTERY

Wanhua Zhao*, Xiaofei Wang*, Yongfei Jiang*and Jun Zhang*

*State Key Laboratory for Manufacturing Systems Engineering
Xianning West Road #28, Xi'an, Shaanxi, China
whzhao@mail.xjtu.edu.cn

Key words: Stent, CFD, Curved artery, Non-Newtonian, Wall Shear Stress

Abstract. *In stented arteries, regions exposed to low wall shear stress are prone to intimal hyperplasia, which is the main reason for restenosis. The distributions of wall shear stress(WSS) are very important predictors for a stent's potential performance. Some previous studies showed that the implantation of stent changed the geometry of the artery and thus affected the distributions of WSS. In other studies, straight artery models were employed to evaluate the fluid characteristics of particular stents. However, all of the previous studies ignored either the non-Newtonian behavior of the blood or the local curvature of the arteries. We compared Newtonian and non-Newtonian blood flows in an average curved coronary artery implanted with a stent through computational fluid dynamic approach. The results indicated that the viscosity thinning behavior of blood was the dominate factor of the variations of WSS when the average flow velocity was low, while the geometry of the artery dominated the variations of WSS when the average flow velocity was high.*

1 INTRODUCTION

Characterized by hardening and remodeling of the arterial wall, atherosclerosis make the arterial segments suffering from this disease occluded. The consequential insufficiencies of blood supply to the distal tissues, for example in brain and heart, lead to strokes and heart attacks respectively. Either of these diseases is disabling or killing a large number of people every year. Nowadays, stents are widely used to prop open the diseased arteries after percutaneous transluminal angioplasty. However, the incidence of restenosis, which is the re-narrowing of the lesions, can reach to 20-40% after the implantation of bare metal stents[1]. Although the drug eluting stents can reduce restenosis to about 5%[2, 3], the risk of in-stent thrombotic increased due to the delayed re-endothelializaion[4-6]. Therefore, more approaches are needed to reduce the restenosis while keeping the adverse by-effects as small as possible.

Autopsy results indicated that about 3 months later after the implantation of stents, a new layer of intima formed above the strut of the stents. The hyperplasia of this neointimal layer, which is mainly composed of smooth muscle cells, lead to restenosis[7]. Some studies revealed that the neointima thickness closely correlate with the density of inflammatory cells[8, 9]. Increased WSS is accompanied by the reduction in neointimal hyperplasia[10] and a local reduction in inflammation[11]. These studies indicated that high WSS may reduce neointima formation through inhibition of inflammation. Thus, it is crucial to simulate the values of WSS in the stented arteries in the prediction of the potential performance of particular stent designs.

To evaluate the hemodynamic characteristics of stent, investigaters proposed and studied many parameters of stents which include the thickness of the strut[12, 13], the strut profile[13], the geometric structure of the strut[14], the shape and number of strut-strut connectors[14], the strut-strut spacing[14, 15] and the deployment ratio[16]. However, almost all of these studies assumed that the stents were implanted into straight cylindrical arteries, while in reality the atherosclerosis are prone to tortuous arterial segments and bifurcations. The implantation of the stents changed the 3-D geometry of the arteries and thus changed the distributions of WSS which may contribute to the inhomogeneous distributions of in-stent neo-intima[17]. Moreover, the rheological behavior of blood was usually assumed to be Newtonian. The distributions of WSS induced by non-Newtonian blood flow in curved stented arteries were not well known. Thus we simulated the Newtonian and non-Newtonian blood flow in an ideally curved stented artery and compared the variations of WSS induced by the curvature of the artery between the two computational models of blood flow.

2 MOTHODS

In order to study the influence of curvature on the distribution of WSS in a generic sense, we did not construct a patient specific stented artery. Instead, we constructed an ideally curved artery supported by a stent which conformed to the curvature. The diameter of the artery was 3.6mm; the curved segment was 20mm; and the length of stent was 12mm. The curvature radius was 7.85m, which was similar with those of some swine coronary arteries measured in the study performed by Wentzel et.al.[17]

The stent was comprised of sinusoidal supporting bodies connected with "v" structures. One 10mm long straight tube was attached to the proximal and distal ends of the stented segment, respectively, in order to ensure a fully developed velocity profile and remove the exit effects(Figure 1). The blood was assumed to be homogeneous fluid with a density of 1060kg/m^3. For the simulation of Newtonian blood flow, the viscosity was set to 3.5cP. The inlet velocity was determined through the approach described in literature[14]. Finally, the low and high inlet flow velocities were set to 0.06m/s and 0.15m/s so that the WSS in straight segment was 0.5Pa and 1.5Pa respectively, which were observed in arteries under normal physiologic conditions.

For non-Newtonian blood flow in human arteries, the viscoelastic properties can be ignored safely[18]. The viscosity thinning behavior was described with Carreau model

$$\mu = \mu_\infty + (\mu_0 - \mu_\infty)[1 + (\lambda\dot{\gamma})^2]^{(n-1)/2}$$

where λ is the time constant; n is the power-law index, μ_0 and μ_∞ are the zero and infinite shear viscosities respectively. All of these parameters used in this study were identical with those used in literature[19].

$$\lambda = 3.313\text{s}, n = 0.3568, \mu_0 = 5.6\text{c}P, \mu_\infty = 0.345cP$$

The Re number was 65~164($Re = \rho\upsilon D/\mu$) <<2300, which means the blood flow was laminar flow. In curved tube，the De number is given by

$$De = Re\sqrt{(D/2*C)}$$

Where D is the diameter of the tube， C is the curvature of the center line respectively. In this case, the value of De was 7.72~19.49. The computational zones were governed by the Navier-Stokes and continuity equations. No-slip velocity boundary conditions were defined on the walls and a pressure outlet condition was imposed on the outlet with uniform pressure of 0 Pa.

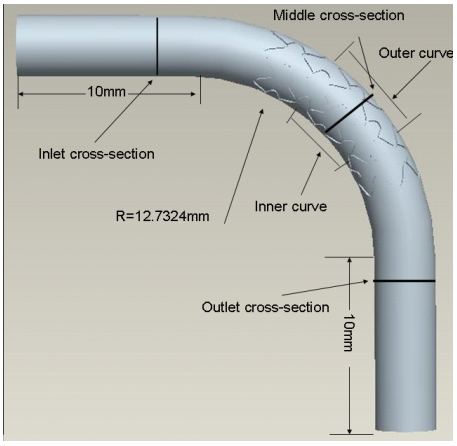

Figure 1: Three-dimensional model of the stented artery

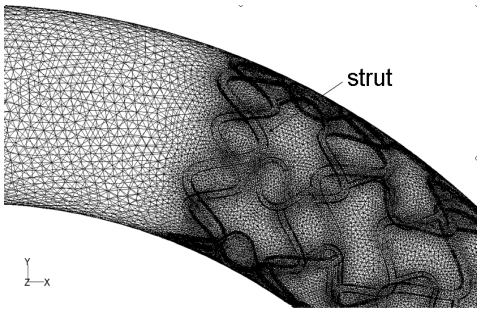

Figure 2: Computational grid of the stented artery.

The grid near the strut was intensified to obtain more precise results in these interested zones(Figure 2). The convergence criteria of continuity and velocity residuals were all set to 10e-5. For non-Newtonian flow simulation, the convergence criteria of energy residual were set to 10e-6. Besides, two points were set at the inlet segment to monitor the value of WSS. When both the convergence criteria of residuals were met and the lines of WSS in the monitor windows were leveled, the computations were thought to be converged. The grid nodes were doubled and the values of WSS at the inlet segment varied within 5%, which mean the criteria of grid independence was met[15]. All of these computations were done on the HPxw6600 workstation.

3 RESULTS

3.1 The distribution of velocity magnitude

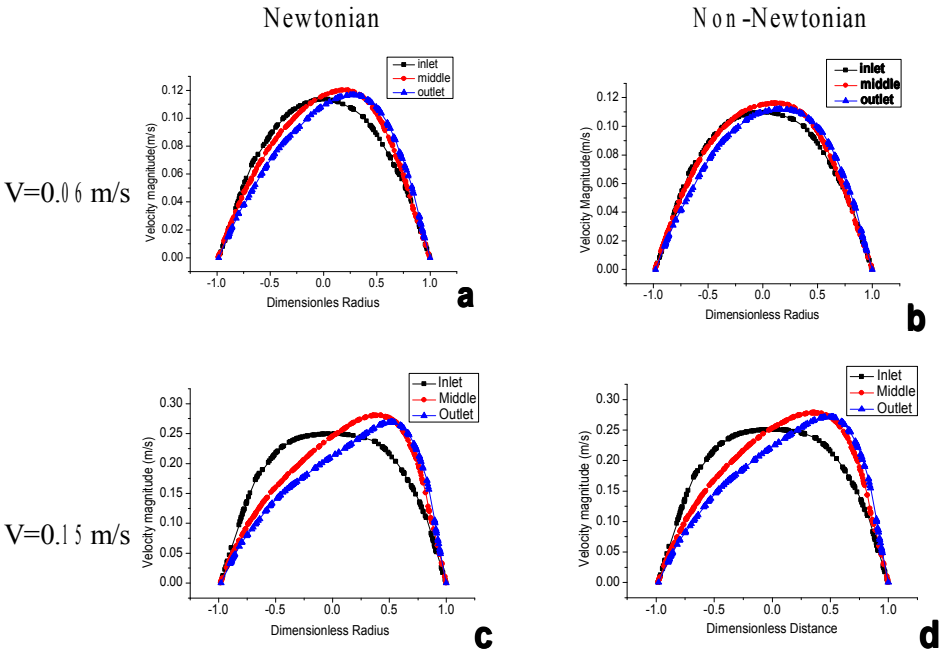

Figure 3: Velocity profiles in the inlet, middle and outlet cross-sections.

When the average flow velocity was low, the velocity profile was parabolic and the peak of the velocity profile skewed slightly to the outer curve (Figure 3 a, b). Compared with that for the Newtonian blood flow, the velocity peak for the non-Newtonian blood

flow was lower and the skewing was smaller. These results agreed well with the results obtained from the numerical simulations of Newtonian and non-Newtonian blood flows in carotid bifurcation models[20]. The non-Newtonian behavior of the blood dampened the shift of the peak axial velocity. As the average flow velocity increased, the boundary layer became thinner, and central region of the velocity profile became flatter (Figure 3 c, d). The skewing to the outer curve became very considerable, leading to higher shear rates in the outer curve. To the contrary, the differences of velocity profile between the Newtonian and non-Newtonian blood models became smaller.

3.2 The distribution of dynamic viscosity

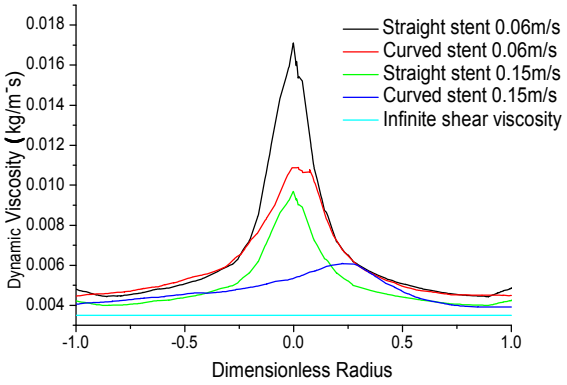

Figure 4: Profiles of dynamic viscosities in the middle cross-section at deferent conditions.

The dynamic viscosities of the blood under all conditions became nearly constant at the vicinity of the wall (Figure 4). The viscosities were approximately 4cP, instead of 3.5cP, named infinite shear value. As the average flow velocity increased, the dynamic viscosities near the wall changed slightly. The peak of the viscosities also shifted to the outer curve. This was due to that the shear rates at the peak of velocity profile were low. In the bulk of the blood flow near the centerline, the viscosity was much higher than 3.5cP. Gijsen et al.[18] and Benard et al.[21] identified similar phenomena respectively.

3.3 The distribution of WSS

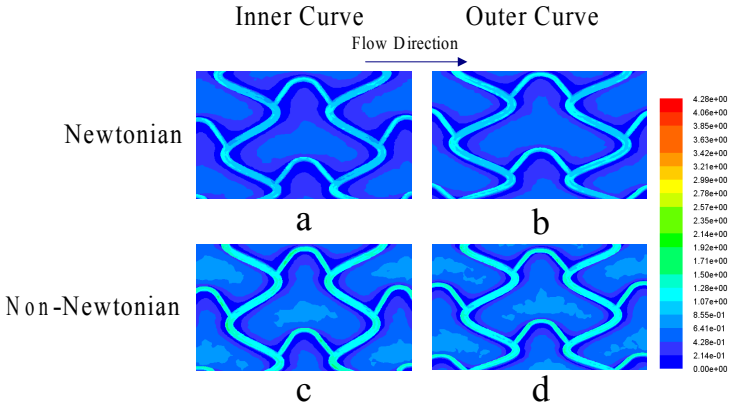

Figure 5: Contour plots of WSS magnitude values for
(a) Newtonian blood flow, inner curve; (b) Newtonian blood flow, outer curve;
(c)non-Newtonian blood flow, inner curve; (d)non-Newtonian blood flow, outer curve. (V=0.06m/s)

When the average flow velocity was 0.06m/s, the WSS magnitude values were 0.5Pa at the unstented arterial segments (Figure 5 and Figure 6). The changes of WSS distributions due to the employment of stents could be seen in Figure5 and Figure 6. The highest values of WSS (nearly 1.5Pa) were reached at the top of struts. The lowest values were located at the immediate vicinity of the struts. And the values of WSS were increasing at in the directions toward to the center of the stent cells. The average WSS for the non-Newtonian blood flows were 30% and 25% higher compared with those for the Newtonian blood flows on the inner curve and outer curve respectively. The average WSS were 10% higher on the outer cure than on the inner curve for the Newtonian blood flow and 5.8% for the non-Newtonian blood flow.

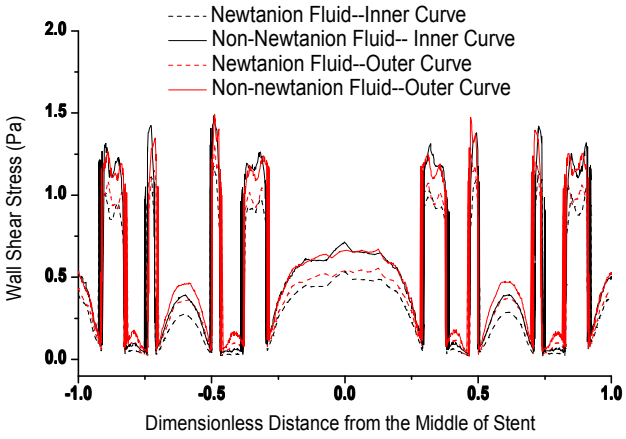

Figure 6: Profiles of WSS in the middle lines of the inner and outer curves in the stented artery (V=0.06m/s).

When the average flow velocity was 0.15m/s, the differences of average WSS between the inner curve and the outer curve increased to 65.2% for Newtonian flow and 59.4% for non-Newtonian flow(Figure 7 and Figure 8). To the contrary, the differences of average WSS between the non-Newtonian and the Newtonian flow decreased to 7.6% on the inner curve and 4.6% on the outer curve respectively.

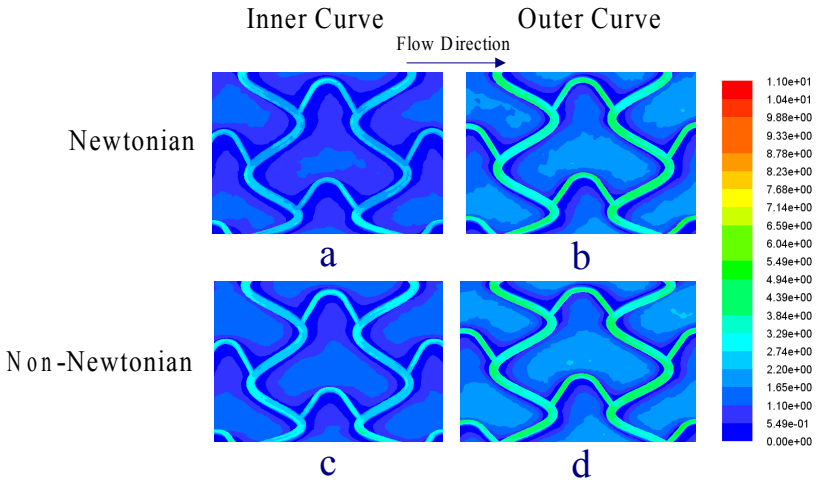

Figure 7: Contour plots of WSS magnitude values for (a) Newtonian blood flow, inner curve; (b) Newtonian blood flow, outer curve; (c)non-Newtonian blood flow, inner curve;(d)non-Newtonian blood flow, outer curve.(V=0.15m/s)

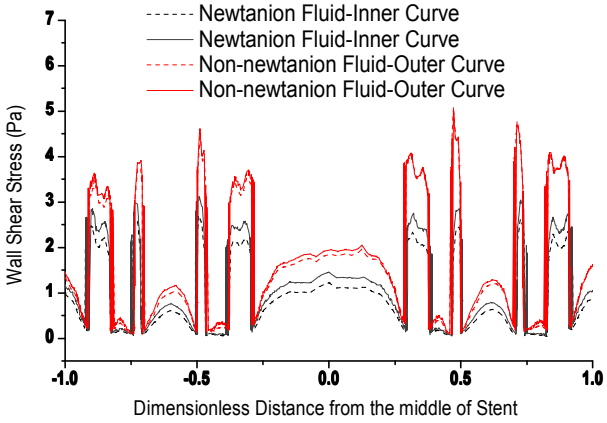

Figure 8: Profiles of WSS in the middle lines of the inner and outer curves in the stented artery (V=0.15m/s).

Average velocity	Inner Curve		Outer Curve	
	Newtonian	Non-Newtonian	Newtonian	Non-Newtonian
0.06m/s	0.40pa	0.52pa	0.44pa	0.55pa
0.15m/s	0.92pa	1.01pa	1.52pa	1.61pa

Table 1: Average WSS Along the Middle Line of the Two Curves.

4 DISCUSSIONS

Computational fluid dynamics (CFD) is widely used to investigate the blood flow in stented arteries, because it can provide quantitative information about the flow field. Straight cylindrical artery models were employed to evaluate the hemodynamic parameters of different stent designs through CFD approach[12, 14, 16, 22]. The distribution patterns of WSS for Newtonian blood flow in straight arterial segments in this study agreed well with those parameters derived from previous studies. The skewing patterns of the axial velocity profile agreed well with the data obtained from experimental and computational studies in a carotid bifurcation model for both Newtonian and non-Newtonian models[18].

The argument for the assumption of Newtonian properties of blood in previous studies is that when the shear rate is above 100/s, the viscosity becomes a constant value called infinite shear viscosity. However, stagnant zones occur at the areas proximal and distal to the struts. At these areas the shear rates were far below 100/s and consequently the viscosities were above the infinite shear viscosity. The Newtonian assumption of blood made the arterial areas exposed to low WSS overestimated. When the blood average flow velocity was low, this overestimation was the most significant.

Wentzel et al.[17] and LaDisa et al.[23] studied the straightening effect of stents caused by the axial stiffness of stents. They found that the curvature of arteries increased at the edges of the stents, which resulted in abnormal high and low WSS regions and these regions may have implications for neointimal formation. However, the variations of WSS induced by the normal anatomical arterial geometry were not studied. The present study showed that the values of WSS on the outer curve were higher than the inner curve. These differences were moderate when the average flow velocity was low and were very considerable when the average flow velocity was high. Atherosclerosis is

prone to the inner curve of tortuous arteries, and the low WSS is believed to be one of the dynamic reasons for this phenomenon. The thickness of neo-intima in the inner curve of the stented artery may also be thicker than other areas.

This study imposed a steady blood flow velocity at the inlet instead of a physiologic flow. Since the oscillating WSS is also one of the factors which are associated with the neointimal hyperplasia, further studies with pulsating flow is needed to investigate the temporal variations of WSS. Another limitation of the present study is that we ignored the elasticity of the arterial wall. The compliance of the arterial wall and the stent may lead to a more complex flow field. The third limitation is that we did not construct patient-specific artery models and the arterial geometries at the upstream may cause important changes of hemodynamics in the downstream segments. However, the results can still provide some useful suggestions for the computational modeling of blood flow in the lesions after stentings from a generic perspective.

5 CONCLUSIONS

CFD approach was employed to investigate the distributions of WSS in an ideal curved stented artery. The influence of non-Newtonian behavior of blood and the curvature of the local artery on the variations of WSS were compared under low and high flow velocity conditions respectively. When the average flow velocity was 0.06m/s, for both the Newtonian and non-Newtonian blood flows, the peak of the velocity profile skewed toward to the outer curve slightly, where the values of WSS were a little larger than those on the inner curve. But the differences of WSS between the non-Newtonian and Newtonian blood flows were much larger. When the average flow velocity was 0.15m/s, the skewing of the velocity profile was more considerable. Consequently, the WSS at the outer curve were much larger than those at the inner curve. To the contrary, the differences of WSS between the two blood flow models became smaller.

The protrusion of the stent struts into the lumen caused stagnant or low shear stress regions near the arterial wall, and the effective viscosities at these regions were above the infinite shear stress viscosity. When the blood average flow velocity was low, it seems necessary to assume non-Newtonian blood models to evaluate the distribution of WSS. When the blood average flow velocity was high, the geometry of the artery dominated the variations of WSS.

ACKNOWLEDGMENT

This work is supported by the National Natural Scientific Foundation of China under the grant number: 5775179.

REFERENCE

[1] Kastrati, A., et al., *Restenosis after coronary placement of various stent types.* American Journal of Cardiology, 2001. **87**(1): p. 34-39.

[2] Woods, T.C. and A.R. Marks, *Drug-eluting stents.* Annual Review of Medicine, 2004. **55**: p. 169-178.

[3] Castro, M.A., C.M. Putman, and J.R. Cebral, *Computational fluid dynamics modeling of intracranial aneurysms: Effects of parent artery segmentation on intra-aneurysmal hemodynamics.* American Journal of Neuroradiology, 2006. **27**(8): p. 1703-1709.

[4] Lagerqvist, B., et al., *Long-term outcomes with drug-eluting stents versus bare-metal stents in Sweden.* New England Journal of Medicine, 2007. **356**(10): p. 1009-1019.

[5] Stone, G.W., et al., *Safety and efficacy of sirolimus- and paclitaxel-eluting coronary stents.* New England Journal of Medicine, 2007. **356**(10): p. 998-1008.

[6] Joner, M., et al., *Pathology of drug-eluting stents in humans - Delayed healing and late thrombotic risk.* Journal of the American College of Cardiology, 2006. **48**(1): p. 193-202.

[7] Komatsu, R., et al., *Neointimal tissue response at sites of coronary stenting in humans - Macroscopic, histological, and immunohistochemical analyses.* Circulation, 1998. **98**(3): p. 224-233.

[8] Farb, A., et al., *Morphological predictors of restenosis after coronary stenting in humans.* Circulation, 2002. **105**(25): p. 2974-2980.

[9] Farb, A., et al., *Pathology of acute and chronic coronary stenting in humans.* Circulation, 1999. **99**(1): p. 44-52.

[10] Wentzel, J.J., et al., *Relationship between neointimal thickness and shear stress after wallstent implantation in human coronary arteries.* Circulation, 2001. **103**(13): p. 1740-1745.

[11] Carlier, S.G., et al., *Augmentation of wall shear stress inhibits neointimal hyperplasia after stent implantation - Inhibition through reduction of inflammation?* Circulation, 2003. **107**(21): p. 2741-2746.

[12] Balossino, R., et al., *Effects of different stent designs on local hemodynamics in stented arteries.* Journal of Biomechanics, 2008. **41**(5): p. 1053-1061.

[13] Dehlaghi, V., M.T. Shadpoor, and S. Najarian, *Analysis of wall shear stress in stented coronary artery using 3D computational fluid dynamics modeling.* Journal of Materials Processing Technology, 2008. **197**(1-3): p. 174-181.

[14] He, Y., et al., *Blood flow in stented arteries: A parametric comparison of strut design patterns in three dimensions.* Journal of Biomechanical Engineering-Transactions of the Asme, 2005. **127**(4): p. 637-647.

[15] LaDisa, J.F., et al., *Three-dimensional computational fluid dynamics modeling of alterations in coronary wall shear stress produced by stent implantation.* Annals of Biomedical Engineering, 2003. **31**(8): p. 972-980.

[16] LaDisa, J.F., et al., *Stent design properties and deployment ratio influence indexes of wall shear stress: a three-dimensional computational fluid dynamics investigation within a normal artery.* Journal of Applied Physiology, 2004. **97**(1): p. 424-430.

[17] Wentzel, J.J., et al., *Coronary stent implantation changes 3-D vessel geometry and 3-D shear stress distribution.* Journal of Biomechanics, 2000. **33**(10): p. 1287-1295.

[18] Gijsen, F.J.H., et al., *The influence of the non-Newtonian properties of blood on the flow in large arteries: unsteady flow in a 90 degrees curved tube.* Journal of Biomechanics, 1999. **32**(7): p. 705-713.

[19] Johnston, B.M., et al., *Non-Newtonian blood flow in human right coronary arteries: steady state simulations.* Journal of Biomechanics, 2004. **37**(5): p. 709-720.

[20] Gijsen, F.J.H., F.N. van de Vosse, and J.D. Janssen, *The influence of the non-Newtonian properties of blood on the flow in large arteries: steady flow in a carotid bifurcation model.* Journal of Biomechanics, 1999. **32**(6): p. 601-608.

[21] Benard, N., R. Perrault, and D. Coisne, *Computational approach to estimating the effects of blood properties on changes in intra-stent flow.* Annals of Biomedical Engineering, 2006. **34**(8): p. 1259-1271.

[22] Duraiswamy, N., R.T. Schoephoerster, and J.E. Moore, *Comparison of Near-Wall Hemodynamic Parameters in Stented Artery Models.* Journal of Biomechanical Engineering-Transactions of the Asme, 2009. **131**(6): p. -160.

[23] LaDisa, J.F., et al., *Alterations in regional vascular geometry produced by theoretical stent implantation influence distributions of wall shear stress: analysis of a curved coronary artery using 3D computational fluid dynamics modeling.* Biomedical Engineering Online, 2006. **5**: p. -.